VIROLOGY 245, 75–89 (1998)
ARTICLE NO. VY989154

Mutations in Viral Movement Protein Alter Systemic Infection and Identify an Intercellular Barrier to Entry into the Phloem Long-Distance Transport System

Hong-Li Wang,* Yi Wang,* Donna Giesman-Cookmeyer,†[1] Steven A. Lommel,† and William J. Lucas*,[2]

*Section of Plant Biology, University of California, Davis, California 95616; and †Department of Plant Pathology, North Carolina State University, Raleigh, North Carolina 27695-7616

Received January 5, 1998; returned to author for revision February 2, 1998; accepted March 18, 1998

Viral systemic infection of a plant host involves two processes, cell-to-cell movement and long-distance transport. Molecular determinants associated with these two processes were probed by investigating the effects that alanine scanning mutations in the movement protein (MP) of red clover necrotic mosaic virus (RCNMV) had on viral infection in the plant hosts *Nicotiana edwardsonii, Vigna unguiculata* (cowpea), and the experimental plant *Nicotiana benthamiana.* Plants were inoculated with RCNMV expressing wild-type and mutant forms of the MP. Immunocytochemical studies at the light and electron microscope levels were performed on these plants, using a polyclonal antibody raised against the RCNMV capsid protein to identify the cells/tissues that RCNMV could infect. These experiments demonstrated that one cellular boundary at which the RCNMV MP functions to facilitate entry into the phloem long-distance transport system is located at the interfaces between the bundle sheath and phloem parenchyma cells and the companion cell–sieve element complex. Interestingly, in *Nicotiana tabacum,* a host that only allows a local infection, RCNMV cell-to-cell movement was found to be blocked at this same intercellular boundary. Four mutants that were able to systemically infect *N. benthamiana* were partially or completely defective for systemic infection of *N. edwardsonii* and cowpea, which indicated that these MP mutants exhibited host-specific defects. Thus, the roles of the RCNMV MP in cell-to-cell movement and in long-distance transport appear to be genetically distinct. These results are discussed in terms of the mechanism by which RCNMV enters the phloem to establish a systemic infection.

INTRODUCTION

It is generally considered that plant viruses establish an infection by initiating replication in a few individual cells. After a local infection has been established, the virus proceeds to spread within the plant by two distinct mechanisms; cell-to-cell movement into neighboring cells, via plasmodesmata (local infection), and long-distance transport, via the phloem (systemic infection) (Lucas and Gilbertson, 1994; Carrington *et al.,* 1996; Gilbertson and Lucas, 1996). During the systemic infection of a host, the virus often invades and replicates in a number of different plant tissues. For most mechanically transmitted viruses, initial infection typically occurs in epidermal or mesophyll cells. Cell-to-cell movement occurs through the mesophyll until a lower-ordered vein is encountered, at which time the infectious form of the virus must be capable of passage through bundle sheath, vascular parenchyma, and/or companion cells for eventual entry into the sieve elements. Once within the mature functional sieve tube, the virus moves with the phloem translocation stream to distant sink organs, where it may be capable of exiting the phloem to enter and replicate within other phloem and nonphloem tissue.

Cell-to-cell movement of most plant viruses requires a virus-encoded movement protein(s) (MP), but in some cases the viral capsid protein (CP) may also be essential (Atabekov and Taliansky, 1990; Hull, 1991; Maule, 1991; Deom *et al.,* 1992; Lucas and Gilbertson, 1994; Gilbertson and Lucas, 1996). Viral MPs exhibit a number of distinct functions, including RNA binding *in vitro* (Citovsky *et al.,* 1990, 1991; Osman *et al.,* 1992; Schoumacher *et al.,* 1992; Giesman-Cookmeyer and Lommel, 1993), increasing the size exclusion limit (SEL) of plasmodesmata (Wolf *et al.,* 1989; Fujiwara *et al.,* 1993; Noueiry *et al.,* 1994; Waigmann *et al.,* 1994; Ding *et al.,* 1995c; Rojas *et al.,* 1997), and trafficking macromolecules through plasmodesmata (Fujiwara *et al.,* 1993; Noueiry *et al.,* 1994; Waigmann *et al.,* 1994; Ding *et al.,* 1995c; Nguyen *et al.,* 1996; Rojas *et al.,* 1997). Because MP-mediated cell-to-cell transport of viral infectious material is a prerequisite for systemic infection, it has been difficult to determine what role(s), if any, viral MPs may play in long-distance transport that are distinct from those associated with cell-to-cell movement. Even indirect effects of the MP on long-distance transport, such as reducing the efficiency and/or rate of cell-to-cell movement, which could well affect the entry of the infectious form of the virus into the translocation

[1] Present address: U.S. Army Research Office, P.O. Box 12211, Research Triangle Park, NC 27709-2211.

[2] To whom correspondence should be addressed at Section of Plant Biology, Division of Biological Sciences, University of California, Davis, CA 95616. Fax: (530) 752-5410. E-mail: wjlucas@ucdavis.edu.

0042-6822/98 $25.00

stream, remain poorly understood (Dawson and Hilf, 1992; Giesman-Cookmeyer and Lommel, 1993; Hilf and Dawson, 1993).

Plasmodesmal connections between different plant cells (tissues) are not necessarily equivalent and, consequently, the requirements for cell-to-cell movement may not be common across all cell types (Lucas and Wolf, 1993; Lucas, 1995; Waigmann and Zambryski, 1995; Gilbertson and Lucas, 1996; Ghoshroy *et al.,* 1997). For example, it has been shown that expression of the tobacco mosaic virus (TMV) MP in transgenic tobacco plants caused an increase in plasmodesmal SEL between neighboring mesophyll and mesophyll–bundle sheath cells, but had no effect on the plasmodesmata connecting bundle sheath and phloem parenchyma cells (Ding *et al.,* 1992). Additional evidence in support of this hypothesis was provided by studies on a soybean cultivar that is resistant to systemic infection by cowpea chlorotic mottle virus (CCMV). In this host, viral cell-to-cell movement within the mesophyll of inoculated unifoliolate leaves was not impaired (Goodrick *et al.,* 1991). Furthermore, entry into bundle sheath cells was similarly unimpeded. However, the level of CCMV detected within the vascular parenchyma and companion cell–sieve element (CC-SE) complex was greatly reduced, or entirely absent, suggesting that a host factor might be involved in restricting CCMV passage through the plasmodesmata interconnecting bundle sheath and vascular parenchyma cells.

In a study using an attenuated strain of TMV, Ding *et al.* (1995b) also reported a reduction in the levels of TMV within vascular parenchyma and companion cells, which they interpreted as reflecting a delay in cell-to-cell movement of the attenuated TMV strain from the bundle sheath to the vascular parenchyma. Interestingly, for tobacco etch potyvirus (TEV), the barrier to long-distance transport may well be located at the plasmodesmata that interconnect the CC and the SE (Schaad and Carrington, 1996). Based on these collective observations, we hypothesize that viral MPs possess separate functional motifs essential for cell-to-cell movement of the viral genome across specific tissue barriers or domains (see Wang *et al.,* 1996; Sudarshana *et al.,* 1998).

In the present study, we employed previously described alanine scanning mutations in the MP of red clover necrotic mosaic virus (RCNMV) (Fujiwara *et al.,* 1993; Giesman-Cookmeyer and Lommel, 1993) to test this hypothesis. Using this viral system, we were able to establish that specific mutations in the RCNMV MP inhibited, or abolished, viral movement from bundle sheath and/or phloem parenchyma cells into the CC-SE complex within inoculated leaves. Our studies also demonstrated that the RCNMV MP is required for efficient long-distance transport of RCNMV in *Nicotiana edwardsonii* and *Vigna unguiculata* (cowpea), in contrast to the situation in *Nicotiana benthamiana,* where all RCNMV MP mutants were capable of establishing a systemic infection. The role of the MP in this process was genetically distinct from its known functions in cell-to-cell movement within mesophyll tissue. The same cellular barrier to RCNMV movement was identified using *Nicotiana tabacum,* a host that naturally restricts infection by wild-type RCNMV to the inoculated leaf. These results are discussed in terms of the manner in which the RCNMV MP and CP might interact to facilitate RCNMV entry into and exit from the phloem long-distance transport pathway.

RESULTS

Host range of RCNMV MP mutants

A number of RCNMV MP alanine scanning mutants (27–31, 204, 242, 301, 305, and double mutant 27–31/305) were analyzed for their ability to systemically infect plant hosts in addition to *N. benthamiana.* An additional mutant, RCNMV MP mutant 280, which reverts rapidly to wild type on *N. benthamiana,* was included in this host range analysis to determine whether it would also display the same rapid reversion to wild type in other plant hosts. RCNMV MP mutant 280 is partially functional in that it is able to increase plasmodesmal SEL, but is incapable of trafficking RNA from cell to cell (Fujiwara *et al.,* 1993). Thus, this mutant is restricted to the initially inoculated cells, but, if during replication a reversion to wild type occurs, it can then move from cell to cell and long distance (Sit and Lommel, unpublished results; Giesman-Cookmeyer and Lommel, 1993).

All of the wild-type and mutant viruses tested (with the exception of 280, see below) moved cell to cell and induced symptoms on the inoculated leaves of *N. edwardsonii* and cowpea (data not shown). Wild-type virus and mutant viruses 242 and 301 also induced symptoms on the uninoculated (upper) leaves and caused systemic infections in both hosts; as a consequence they were not further studied. Two of the RCNMV MP mutants, 27–31 and 204, and the double mutant 27–31/305, did not induce symptoms on the upper leaves of *N. edwardsonii.* RCNMV mutant 305 induced symptoms on the upper leaves of 25% of the inoculated *N. edwardsonii* plants (Table 1). One case of a reversion was observed for RCNMV MP mutant virus 280 inoculated onto six *N. edwardsonii* plants, which resulted in the development of a systemic infection (Table 1). In the one instance where mutant virus 280 reverted to wild type and caused a systemic infection in *N. edwardsonii,* viral RNA was detected in the upper leaves. This viral RNA was sequenced and it was confirmed that the original mutation had reverted to wild type (data not shown). In all other *N. edwardsonii* and cowpea plants infected with mutant virus 280, symptoms did not appear on either the inoculated or upper leaves. In cowpea, mutants 27–31 and 305, and the double mutant 27–31/305, did not induce

TABLE 1

Ability of RCNMV and Seven MP Alanine Scanning Mutants to Systemically Infect Three Systemic Hosts, *Nicotiana edwardsonii, Vigna unguiculata,* and *Nicotiana benthamiana*

RCNMV MP mutants	Inoculated plants[a]		
	N. edwardsonii	*V. unguiculata*	*N. benthamiana*
WT	16 (16)[b]	16 (16)	16 (16)
27–31	0 (16)	0 (16)	16 (16)
204	0 (16)	2 (16)	16 (16)
242	6 (6)	6 (6)	6 (6)
280	1[c] (6)	0 (6)	1[c] (6)
301	6 (6)	6 (6)	6 (6)
305	4 (16)	0 (16)	16 (16)
27–31/305	0 (16)	0 (16)	16 (16)

[a] Data are based on either the appearance of symptoms or the presence or absence of viral genomic RNA in the upper uninoculated leaves of infected plants 21 dpi. A positive correlation was observed between the appearance of symptoms and the presence of viral RNA (data not shown). Symptoms appeared on the inoculated leaves of *N. edwardsonii* and *N. benthamiana* at 4–5 and 3–4 dpi on cowpea for wild-type RCNMV. For inoculations with RCNMV expressing mutant MPs, only mutant MP 27–31 and mutant MP 27–31/305 had delays in the appearance of symptoms on the inoculated leaves; the delays were 1–2 days for all plants tested. Lesions that developed on inoculated leaves of cowpea that were caused by mutant MP 27–31 and mutant MP 27–31/305 were much smaller than those caused by the wild-type RCNMV or any of the other RCNMV mutant MPs tested.

[b] Values indicate the number of plants exhibiting systemic symptoms and accumulation of viral RNA; values in parentheses indicate the total number of plants inoculated in each experiment.

[c] Single *N. benthamiana* and *N. edwardsonii* plants that became systemically infected by RCNMV MP mutant 280 were the result of reversion mutations.

symptoms on the upper leaves. In addition, mutant 204 induced symptoms on the upper leaves in only 13% of the inoculated cowpea plants. These data indicate that mutations in the RCNMV MP can restrict viral movement to the inoculated leaves of two systemic hosts, *N. edwardsonii* and cowpea.

As indicated in Table 1, all RCNMV MP mutants, with the exception of mutant 280, were capable of establishing local and systemic infections on inoculated *N. benthamiana* plants. This suggested that the host-specific defects in MP function(s) that were responsible for restricting virus movement in *N. edwardsonii* and cowpea either were absent or were overcome by the mutant MPs in *N. benthamiana.* Another important observation resulting from these infection studies was that even though mutants 204 and 305 failed to move systemically in *N. edwardsonii* and cowpea, at wild-type levels, cell-to-cell movement of these mutants was not severely impaired within inoculated leaves (see Figs. 1D and 1F). Symptoms appeared on the inoculated leaves at the same time for the wild-type virus and mutant viruses 204 and 305 for all plants tested. This was not the case for mutant viruses 27–31 and 27–31/305, where, compared with wild-type RCNMV, a delay of 1–2 days was observed in the appearance of symptoms on inoculated leaves of *N. edwardsonii* and cowpea, whereas for *N. benthamiana,* symptom development was the same as observed with wild-type RCNMV (Table 1).

To ensure that systemic infection was not occurring in the absence of symptom development, Northern blot hybridization analyses were performed on the upper leaves of inoculated plants. These studies demonstrated that there was always a positive correlation between the appearance of symptoms in upper uninoculated leaves and the presence of viral RNA; in no case was viral RNA detected in leaf samples taken from inoculated plants which failed to exhibit systemic symptoms (data not shown). Furthermore, except for the case of mutant 280, the development of systemic symptoms on plants inoculated with these RCNMV MP mutants was not due to a reversion. This was established by sequencing the progeny viruses extracted from plants systemically infected with each mutant virus; in these studies the original mutations were still present (data not shown).

Cellular distribution of RCNMV within tissues of inoculated plants

The effects of the mutations in the RCNMV MP on the distribution of mutants 204, 305, 27–31, and 27–31/305 within the tissues of the plant were next examined. Plants of *N. edwardsonii* and cowpea were infected with RCNMV expressing either wild-type MP or mutant MPs 204, 305, 27–31, and 27–31/305. Tissue samples were collected from the inoculated leaves 14 dpi and from the upper uninoculated leaves 21 dpi. These samples included the petiole and main vein to the fourth-order veins within the lamina. The presence of RCNMV was detected in the inoculated leaves of *N. edwardsonii* plants using a polyclonal antibody directed against the RCNMV CP. Control experiments performed at the light (fluorescence) microscope level revealed that preimmune serum bound, nonspecifically, to the lignified cell walls of xylem conducting elements (see Fig. 2C). A similar, nonspecific, cross-reaction was detected between the RCNMV CP antiserum and the cell walls of the xylem elements (Figs. 1B, 1D, 1F, 1H, 1J, 2B, 2E, and 2F). Immunolabeling experiments performed on *N. edwardsonii* plants inoculated with RCNMV expressing wild-type MP revealed the presence of a strong green fluorescent signal located over all cell types within inoculated leaves. As the RCNMV CP was detected in all cell types, including epidermal, mesophyll, bundle sheath, and phloem cells, these control experiments established that, in this plant host, RCNMV can move cell to cell throughout the tissues of the inoculated leaf. Figure 1B depicts a representative fluorescence micrograph in the region of a second-order vein and Fig. 2B provides a higher magnification view of a fourth-order vein (both tissues infected

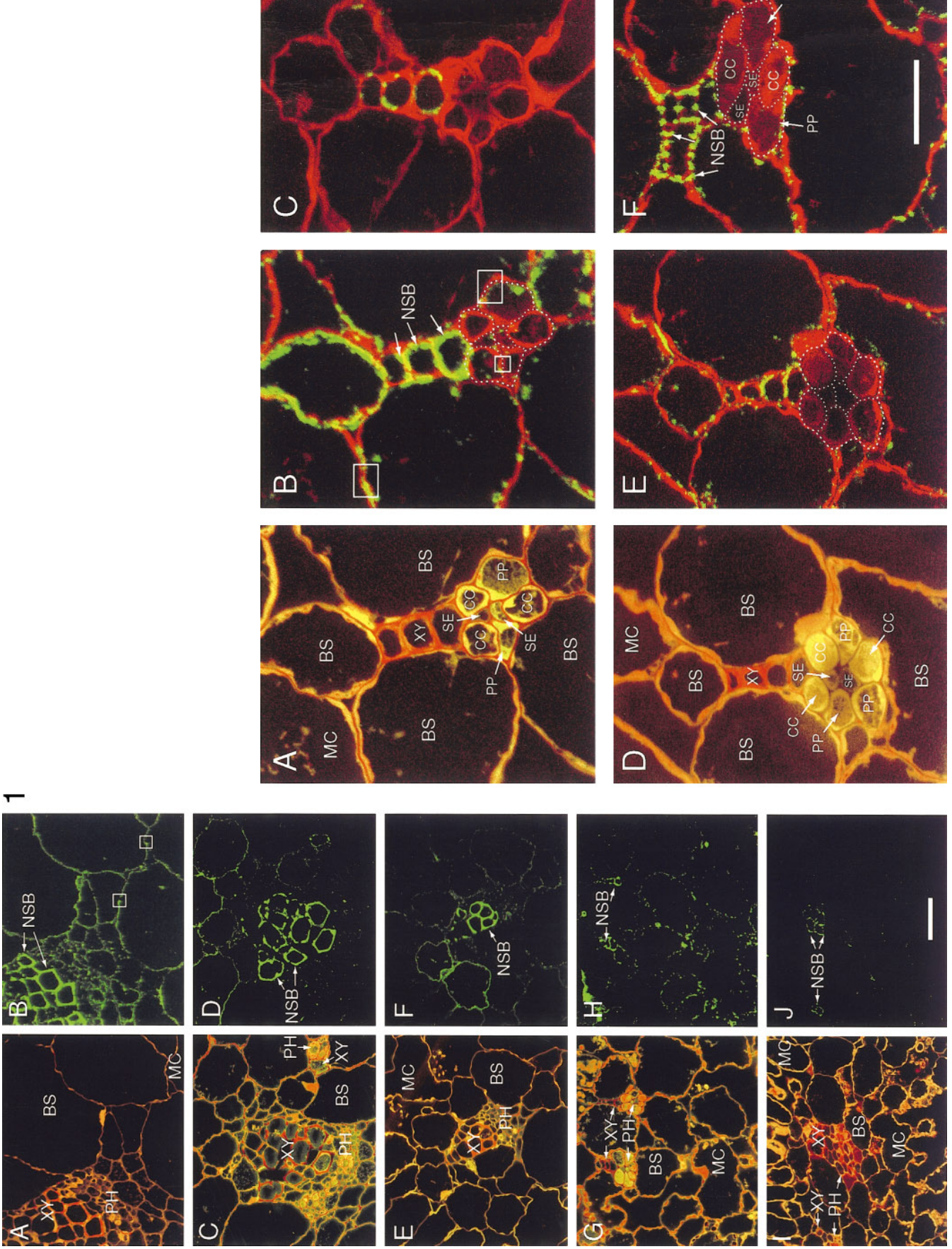
1
A
XY
PH
BS
MC
B
NSB
C
XY
PH
BS
PH
XY
D
NSB
E
MC
BS
XY
PH
F
NSB
G
XY
PH
BS
MC
H
NSB
I
MC
XY
PH
BS
MC
J
NSB
2
A
MC
BS
BS
XY
SE
CC
CC
PP
SE
PP
BS
B
NSB
C
D
MC
BS
BS
XY
CC
SE
CC
PP
PP
SE
CC
BS
E
F
NSB
SE
CC
SE
CC
PP
PP

with wild-type RCNMV). Note the presence of the green ELF signal in the peripheral layer of the cytoplasm; the strong signal detected over the xylem elements represents nonspecific binding of the RCNMV CP antisera to the cell walls. Cellular details associated with these images were gained by imaging the fluorescence associated with Safranin O-stained semiserial sections (cf. Figs. 1A and 2A).

The level of fluorescent signal detected in equivalent leaves inoculated with RCNMV expressing mutant MP 204 (see Fig. 1D) was reduced in all cell types relative to that detected in controls where wild-type RCNMV MP was being expressed (cf. Figs. 1D and 1B). A similar situation was observed with leaves inoculated with mutant MP 305; the level of fluorescent signal was close to that detected for mutant MP 204, but noticeably below the level observed for wild-type RCNMV (cf. Figs. 1F and 1B). For leaves inoculated with RCNMV mutant MP 27–31, the level of fluorescent labeling of the RCNMV CP detected in mesophyll and bundle sheath cells was only slightly less than that observed for wild-type MP, but the level within the phloem was greatly reduced. Figs. 1G and 1H and Figs. 2D–2F illustrate this situation for fourth-order veins; equivalent patterns of fluorescence were observed for all vein orders examined.

These immunofluorescence studies suggested that cell-to-cell spread, from the inoculated epidermal cells to the phloem, by RCNMV expressing mutant MP 204 or 305 is somewhat impaired, whereas for mutant MP 27–31 the main effect appears to be on virus movement into and within the cells of the phloem. Interestingly, fluorescence analysis of leaves inoculated with the double mutant MP 27–31/305 showed that the level of RCNMV CP was greatly reduced in all cell types examined (Figs. 1I and 1J). This demonstrated that infection by RCNMV expressing the double mutant MP 27–31/305 was severely impaired at the level of cell-to-cell movement.

High-resolution immunolocalization studies were next performed, at the electron microscope level, to further confirm the influence of the RCNMV MP mutations on viral movement within inoculated leaves of *N. edwardsonii* plants. As illustrated in Fig. 3, wild-type RCNMV was present at high levels within the cytoplasm of mesophyll (Fig. 3A) and bundle sheath cells (Fig. 3B), and to a lesser extent in phloem parenchyma cells (Fig. 3C). Immunogold labeling was also detected in the CC-SE complex located within all vein orders of the lamina, as well as in the petiole of the inoculated leaf [Figs. 3E (only CC presented) and 3D, respectively]. The cellular/subcellular locations illustrated in these micrographs can be identified from Fig. 1B and Figs. 2A and 2B. A summary of the control experiments obtained on tissue inoculated with wild-type RCNMV is presented in Table 2.

Analyses performed on tissue from *N. edwardsonii* leaves inoculated with either RCNMV mutant MP 204 or 305 confirmed the presence of CP within the cytoplasm of mesophyll, bundle sheath, phloem parenchyma, and CC-SE cells. As indicated by the data presented in Table 2, the RCNMV CP was readily detected in these cells, but at levels below those observed for wild-type RCNMV. Figure 3F illustrates the presence of immunogold label within the CC-SE complex of a third-order vein within a leaf inoculated with RCNMV mutant MP 204. As anticipated from the fluorescence microscopy studies, low levels of immunogold labeling were detected in the phloem tissue of leaves inoculated with either RCNMV MP mutant 27–31 or the double mutant MP 27–31/305 (Table 2). The most significant observation here was that although the RCNMV CP could be detected, sporadically, in phloem parenchyma cells (Figs. 3G and 3H), immunogold label in the CC-SE complex was either absent or present at levels that were only marginally above the level of label detected in preimmune studies (Table 2). Consistent with these observations, neither RCNMV MP mutant 27–31 nor 27–31/305 was detected in the CC-SE within the petioles of inoculated *N. edwardsonii* leaves (Table 2).

Parallel immunogold labeling studies were performed

FIG. 1. Cellular localization of RCNMV within leaves of *Nicotiana edwardsonii* inoculated with RCNMV expressing wild-type and mutant forms of the MP. Sites of RCNMV replication were detected using a combination of a polyclonal antibody raised against the RCNMV CP and enzyme-linked fluorescence (dark green signal). Safranin O staining (red to orange) was used to visualize and identify the cell types within the sections examined. (A and B) Images obtained from a leaf inoculated with RCNMV expressing wild-type MP; (C and D) RCNMV MP mutant 204; (E and F) RCNMV MP mutant 305; (G and H) RCNMV MP mutant 27–31; (I and J) RCNMV MP double mutant 27–31/305. (B, D, F, H, and J) RCNMV CP localization (dark green fluorescence) in transverse sections of leaf tissues within second-order (B and D), third-order (F and J), and fourth-order (H) veins. (A, C, E, G, and I) Cellular arrangement is depicted by a combination of the red and green Safranin O fluorescent channels. Bar, 50 μm. Abbreviations are as follows: BS, bundle sheath; MC, mesophyll cell; NSB, nonspecific binding of CP to xylem conducting cells; PH, phloem; and XY, xylem. Insets in B illustrate typical regions examined using immunogold labeling techniques and electron microscopy; see also Fig. 2B.

FIG. 2. Subcellular localization of RCNMV within leaves of *Nicotiana edwardsonii* inoculated with RCNMV expressing wild-type MP and mutant MP 27–31. Experimental and imaging details are as in Fig. 1. Images obtained from leaves inoculated with RCNMV expressing wild-type MP (A–C) and MP mutant 27–31 (D–F). (A and D) Transverse sections of fourth-order veins visualized by a combination of the red and green Safranin O fluorescent channels. (C) Section immunolabeled with preimmune antisera (combination of Safranin O red fluorescence and green ELF). Note the nonspecific binding of the antisera to the xylem element cell walls. (B, E, and F) Subcellular localization of RCNMV CP visualized by superimposing the green ELF channel onto the red Safranin O fluorescence channel. Dots are employed to highlight location of walls for cells within the vascular tissues. Note that (A) and (B) and (D) and (E) are matching images. Abbreviations are as in Fig. 1 legend, plus CC, companion cell; NSB, nonspecific binding; PP, phloem parenchyma; SE, sieve element. Insets in B illustrate typical regions examined using immunogold labeling techniques and electron microscopy. Representative images are presented from approx. 60 transverse sections examined for each treatment. Bar, 25 μm.

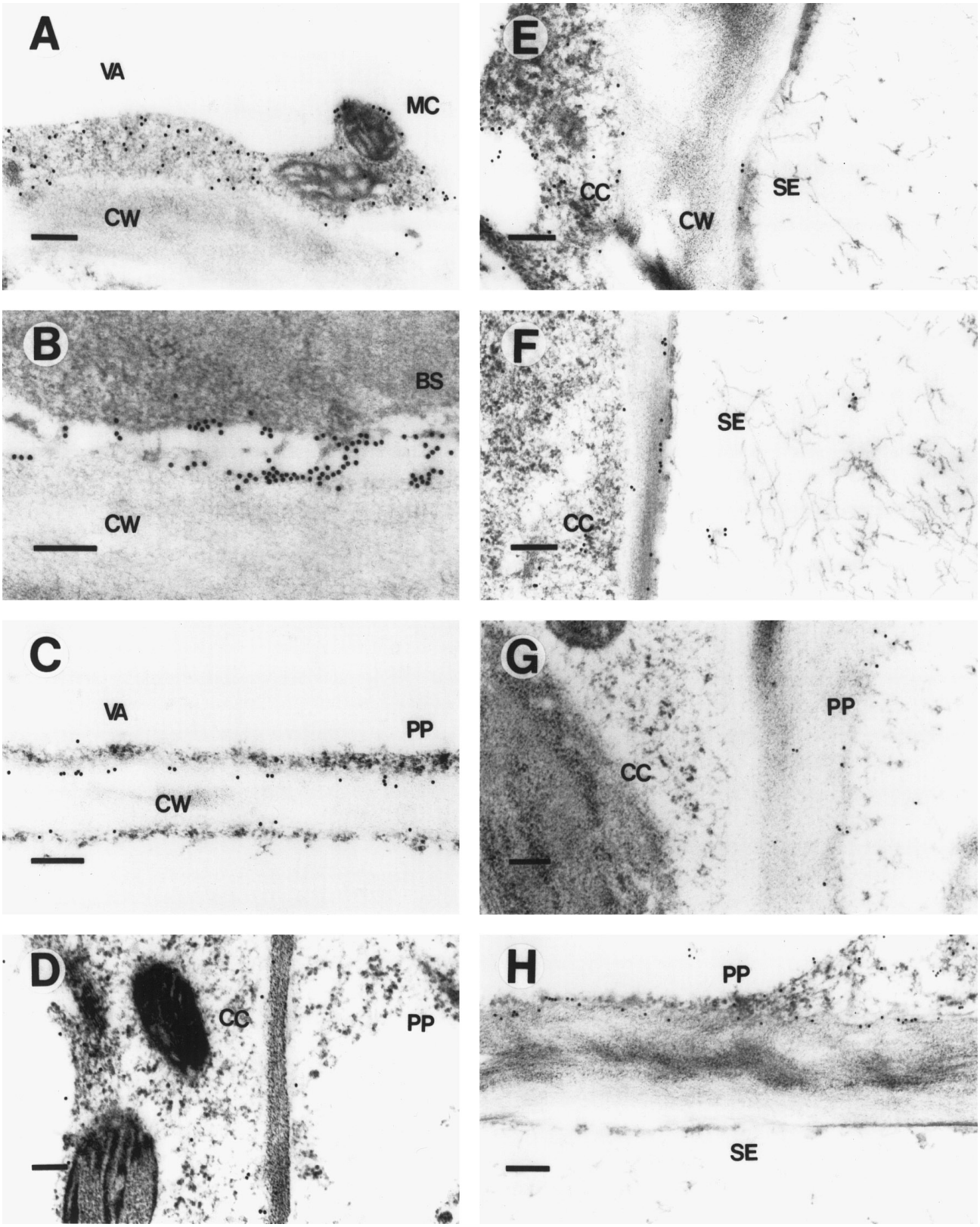

FIG. 3. Subcellular localization by immunogold labeling of RCNMV CP in different cell types of inoculated *N. edwardsonii* leaves that were infected with RCNMV expressing wild-type and mutant forms of the MP (14 dpi). Immunogold labeling was carried out with a polyclonal antibody, raised against the RCNMV CP, and goat anti-rabbit secondary antibody conjugated to 15-nm gold particles. See Fig. 2 for representative sites depicted below. (A–C). Electron micrographs of infected mesophyll, bundle sheath, and phloem parenchyma cells, respectively, located in the lamina of a leaf inoculated with wild-type RCNMV. Note that the immunogold label is confined to the cytoplasm, being absent from the vacuole (VA) and the cell wall (CW). (D) Infected companion cell and phloem parenchyma cell from the petiole of a leaf inoculated with wild-type RCNMV. (E) Infected CC-SE within a fourth-order vein of a leaf inoculated with wild-type RCNMV. (F) Infected CC-SE within a fourth-order vein in a leaf inoculated with RCNMV MP mutant 204. (G and H) Cellular location of RCNMV within a third-order vein in a leaf inoculated with RCNMV MP mutant 27–31. Note the absence of immunogold label in CC and SE. Abbreviations as in legends to Figs. 1 and 2. Bars, 250 nm.

TABLE 2

Analysis of the Cell Types in *Nicotiana edwardsonii* and *Vigna unguiculata* That Were Infected by RCNMV Expressing Wild-Type and Mutant Forms of the MP

RCNMV MP mutants	*N. edwardsonii*						*V. unguiculata*					
	Inoculated leaf (14 dpi)			Upper leaves (21 dpi)			Primary leaf (14 dpi)			Trifoliate leaves (21 dpi)		
	CC-SE[a]	OC	CC-SE*	CC-SE	OC	CC-SE*	CC-SE	OC	CC-SE*	CC-SE	OC	SE-CC*
WT	++[b]	++++	++	++	+++	+	++	++++	++	++	+++	+
204	++	++	+/−	−(+)	−	−(+)	+/−	+++	−(+)	−	−	−
305	++	++	+/−	−(+)	−	−(+)	+/−	+++	−(+)	−	−	−
27–31	−(+)	+++	−	−	−	−	+/−	++	−	−	−	−
27–31/305	−(+)	−(+)	−	−	−	−	+/−	++	−	−	−	−

[a] Cell types examined for the presence of RCNMV: CC-SE, sieve element-companion cell complex; OC, other cells in leaf except CC-SE (mesophyll, bundle sheath, and phloem parenchyma); CC-SE*, in petiole.

[b] Data based on fluorescence microscopy and transmission electron microscopy immunogold cytochemical detection of RCNMV CP. Immunolocalization of RCNMV CP is represented by "+," indicating the presence of virus within the specified cell type. The number of symbols indicates the relative levels of immunofluorescence and gold labeling. Cell types in which CP was not detected in every cell examined have been indicated as follows: +(−), +/−, and −(+), greater than 80%, approx. 50%, and less than 20% of the sections had extremely low, but detectable, levels of immunofluorescence and immunogold labeling, respectively. Cells in which CP was not detected are indicated by −.

on inoculated primary leaves of cowpea. Wild-type RCNMV produced abundant levels of RCNMV CP in mesophyll, bundle sheath, and phloem parenchyma cells (Figs. 4A–4C). However, the extent of immunogold labeling detected in the CC-SE complex was appreciably less than that observed in other cell types within the inoculated primary leaf (compare Fig. 4E with Figs. 4A–4C; note also the absence of labeling within the CC-SE complex in the preimmune experiment depicted in Fig. 4D). The infection pattern that developed when cowpea primary leaves were inoculated with RCNMV MP mutants 204 and 305 was similar to wild-type RCNMV, in that these MP mutants were able to replicate in and move among mesophyll, bundle sheath, and phloem parenchyma cells. However, the extent of immunogold labeling in these cell types was approximately half that detected in leaves inoculated with wild-type RCNMV (Table 2).

It is important to note that in cowpea, entry into the CC-SE complex appeared to be inhibited for both MP mutants 204 and 305. When detected, the level of immunogold label in the CC-SE complex of the third- and fourth-order veins was sparse (Table 2 and Fig. 4F). Analysis of the phloem located within the petiole of primary leaves inoculated with either RCNMV MP mutant 204 or 305 revealed that the CP was present in the CC-SE complex at levels well below those measured for tissue infected with wild-type RCNMV (Table 2). Finally, based on immunocytochemical studies, RCNMV MP mutants 27–31 and 27–31/305 were able to replicate and move within the mesophyll, bundle sheath, and phloem parenchyma of cowpea primary leaves, but movement appeared to be impaired, as the level of immunogold label was approximately 50% that detected in tissue inoculated with wild-type RCNMV (Table 2). These same RCNMV MP mutants also appeared to be inhibited in terms of their ability to enter the CC-SE complex, in that less than 50% of the CC-SE examined showed any evidence of immunogold labeling (Fig. 4G). Furthermore, label was not detected in the CC-SE complex of the petiole (Table 2).

Studies were next performed on upper, systemically infected, leaves of *N. edwardsonii* and cowpea plants to identify the cellular distribution of RCNMV expressing wild-type and mutant forms of the MP. A combination of light and electron microscopic analyses were employed and a general summary of the results from these studies is presented in Table 2. At 21 dpi, RCNMV expressing wild-type MP had moved long distance, via the phloem, into the upper leaves of *N. edwardsonii,* where the CP was readily detected in vascular and mesophyll tissues (Table 2). Examination of second- through fourth-order veins located within such upper infected leaves revealed the presence of immunogold labeling within the CC-SE complex (Figs. 5A and 5B). In contrast, the level of immunogold labeling present within the cells of the upper leaves of plants inoculated with RCNMV MP mutant 204 or 305 was extremely low. Indeed, the RCNMV CP was only detected within a small percentage of the phloem tissues examined (both petiole and the lamina veins). Figures 5C and 5D are representative images collected from CC-SE complexes located within such tissues; in these images there is no evidence for the presence of CP, indeed only on rare occasions were gold particles detected (Table 2). Consistent with the experiments performed on inoculated leaves, both the RCNMV mutants MP 27–31 and 27–31/305 were not detected in any of the tissues located in the upper leaves of *N. edwardsonii* (Table 2).

Experiments performed on upper systemic trifoliolate

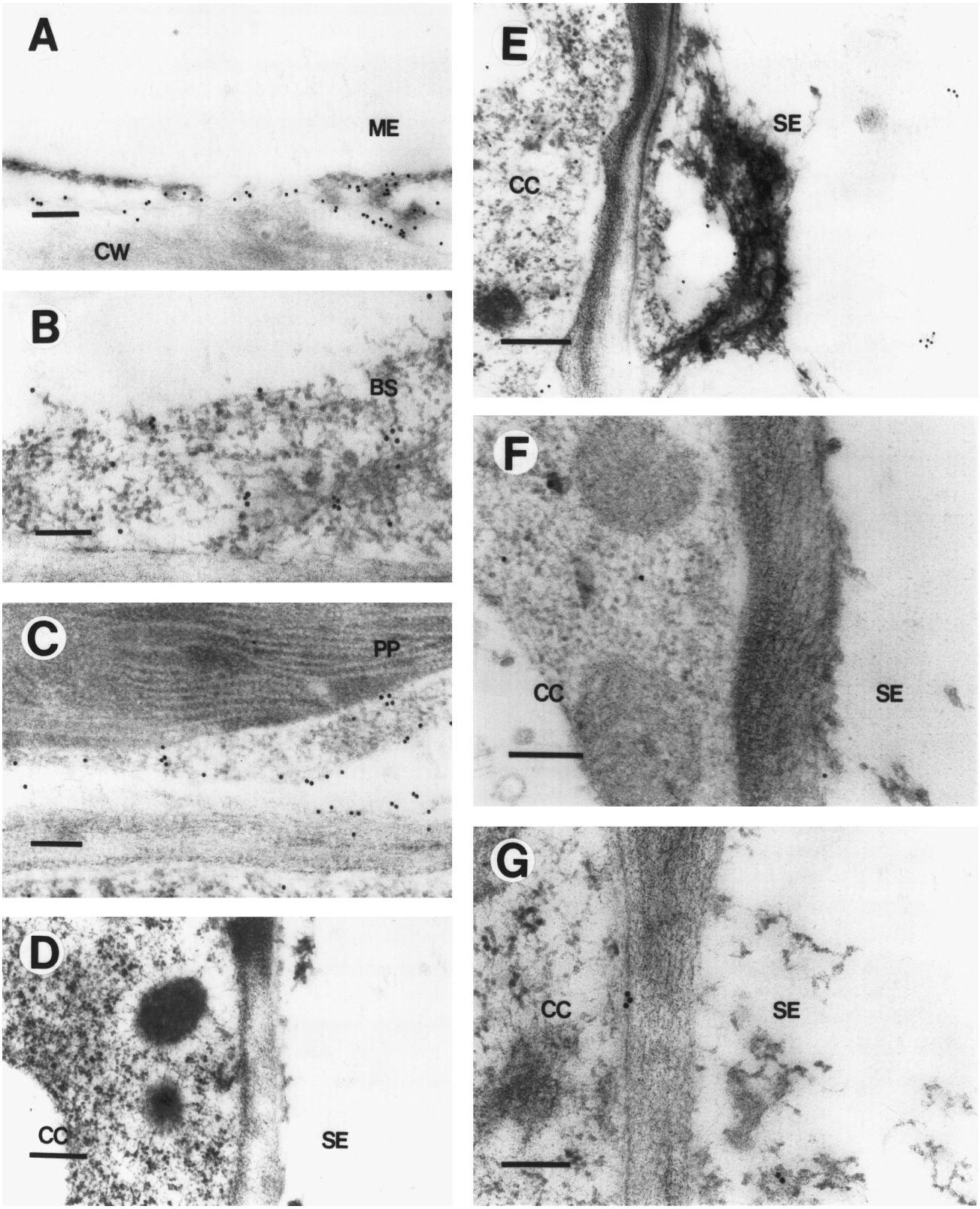

FIG. 4. Subcellular localization of RCNMV CP in different cell types of inoculated cowpea leaves that were infected with RCNMV expressing wild-type and mutant forms of the MP (14 dpi). Immunogold labeling was as in Fig. 3 (note that 15-nm gold was employed in A, D, E, and F and 20 nm gold was used in B, C, and G). (A–C). Electron micrographs of infected mesophyll, bundle sheath, and phloem parenchyma cells, respectively, located in the lamina of a leaf inoculated with wild-type RCNMV. (D) Wild-type RCNMV infected CC-SE (located in a third-order vein) probed with preimmune sera. (E) Infected CC-SE within a third-order vein of a leaf inoculated with wild-type RCNMV. (F and G) Infected CC-SE within a third-order vein in a leaf inoculated with RCNMV MP mutants 305 and 27–31, respectively. Note the low level of immunogold label present in these cell types. Bars, 250 nm, except for D and E (bar, 300 nm).

leaves of cowpea demonstrated that, consistent with symptom development, by 21 dpi wild-type RCNMV had also infected all cell types examined (Table 2 and Figs. 5E and 5F). In cowpea, the contrast between the distribution of RCNMV CP in the trifoliolate leaves of plants infected with wild-type and MP mutant viruses was even more dramatic than that observed for upper systemic leaves of *N. edwardsonii.* All trifoliolate tissues examined from plants inoculated with RCNMV MP mutants 204, 305, 27–31, and 27–31/305 were found to be completely free of immunogold label (Table 2 and Figs. 5G and 5H; see also Table 1).

Immunogold labeling studies were next perfomed on inoculated plants of *N. benthamiana.* Wild-type RCNMV, as well as all of the RCNMV MP mutants, were readily detectable in all cell types of both the inoculated (14 dpi) and upper leaves (21 dpi) of these *N. benthamiana* plants (data not shown). These findings were as expected, as all of the RCNMV MP mutant strains were shown to establish systemic infections on *N. benthamiana* (Table 1; Giesman-Cookmeyer and Lommel, 1993). Thus, in *N. benthamiana,* the boundary between the bundle sheath and/or the phloem parenchyma and the CC-SE complex does not appear to impose the same barrier to RCNMV MP mutant function, in terms of MP-mediated viral entry into the phloem long-distance transport system.

Infection pattern in a nonsystemic host for RCNMV

It has previously been established that RCNMV is capable of infecting *N. tabacum* cv. Xanthi plants, but replication is restricted to inoculated leaves (Ragetli and Elder, 1977). To ascertain the cellular boundary responsible for this confinement, *N. tabacum* plants were infected with wild-type RCNMV and tissue samples were collected from the inoculated leaves 14 dpi and from the upper leaves 21 dpi. Heavy immunogold labeling was detected in mesophyll, bundle sheath, and phloem parenchyma cells within the inoculated leaves (Table 3). Representative images of the immunogold labeling patterns detected within these cell types are presented in Fig. 6. Interestingly, extremely low levels of immunogold label were detected in the CC, and label was never observed in the neighboring SE (Table 3 and Figs. 6D–6F). Consistent with these findings, cells located in tissue samples taken from the upper leaves of such infected plants were completely free of evidence of viral replication/infection. These experiments revealed that the barrier to long-distance transport for wild-type RCNMV, in this nonsystemic host, appears to be the same as that observed for RCNMV MP mutants on systemic hosts.

DISCUSSION

In the present study, seven alanine scanning mutants in the RCNMV MP were employed to further explore the role of the MP in terms of viral entry into and exit from the long-distance transport system of the phloem. Four mutants were identified that were partially or completely defective for systemic infection of *N. edwardsonii* and cowpea, two hosts that support systemic infection by wild-type virus, whereas these same mutants were able to systemically infect *N. benthamiana.* These experiments established that (a) RCNMV MP mutants can exhibit host-specific defects, (b) the RCNMV MP is required for viral entry into the phloem for long-distance transport, and (c) its role in this process appears to be genetically distinct from its functions in mediating cell-to-cell movement within the mesophyll, bundle sheath, and phloem parenchyma. The present study also established that an important cellular site at which the RCNMV MP functions to facilitate long-distance transport is located at the boundaries between the bundle sheath and phloem parenchyma and the CC-SE complex.

The infectivity data obtained on *N. edwardsonii* and cowpea plants clearly demonstrated that the RCNMV MP mutants could be divided into three phenotypic classes. The first class, containing MP mutants 242 and 301, was indistinguishable from wild-type RCNMV. In the second class, containing MP mutants 204 and 305, infection and symptom development were observed in inoculated leaves of both hosts. However, MP mutant 204 moved long distance and systemically infected only one-eighth of the cowpea plants and none of the *N. edwardsonii* plants, whereas RCNMV MP mutant 305 moved long-distance and systemically infected one-quarter of the *N. edwardsonii* plants, but none of the cowpea plants. The third class, containing MP mutants 27–31 and 27–31/305, was competent to infect cells within the inoculated leaves of both *N. edwardsonii* and cowpea plants, but neither moved long distance in, nor systemically infected, these two plant hosts.

The immunofluorescence and immunogold labeling studies provided important insights into the basis for these phenotypic classes of infection. In the third and most severely affected class, RCNMV CP was very rarely detected in the CC-SE complex of second- through fourth-order veins within inoculated leaves of *N. edwardsonii* and cowpea, and never in the CC-SE complex of the petiole (Table 2). This indicates that these MP mutants, although able to move with varying degrees of efficiency from cell to cell in all three hosts, and long distance in *N. benthamiana* plants, are severely impaired in their ability to move through the plasmodesmata that interconnect both bundle sheath and phloem parenchyma cells to the CC-SE complex (Figs. 1 and 2). In this phenotypic class, neither RCNMV MP mutant was detected within any cell type in tissue from the upper leaves of infected *N. edwardsonii* or cowpea plants. Hence, RCNMV MP mutants 27–31 and 27–31/305 may also be impaired in long-distance transport. The present data cannot be used to distinguish between these viral MP mutants having a

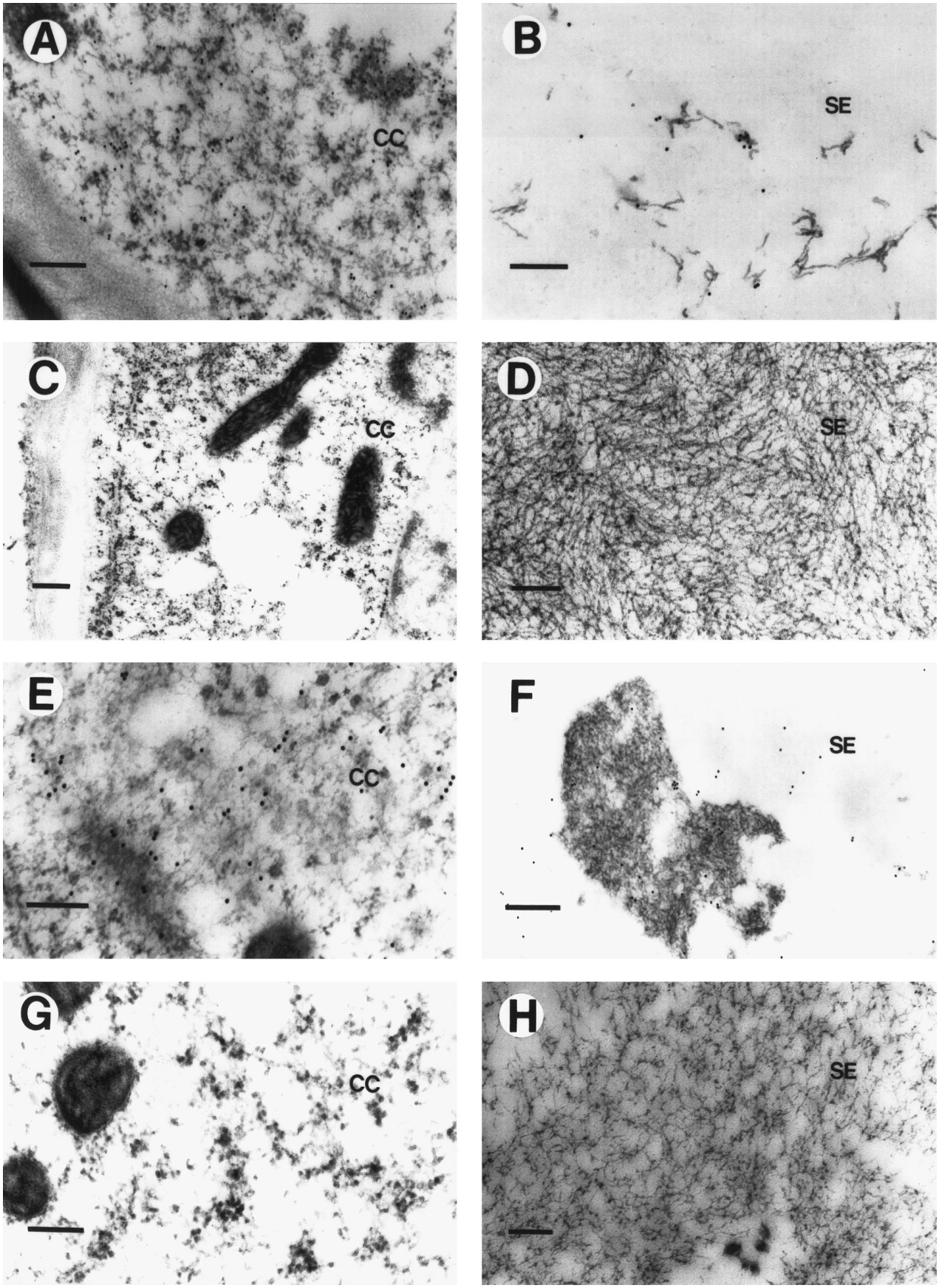
A
CC
B
SE
C
CC
D
SE
E
CC
F
SE
G
CC
H
SE

defect in cell-to-cell movement across either the bundle sheath– or phloem parenchyma–CC boundary that, indirectly, prevents long-distance transport, or having two distinct defects, one in cell-to-cell movement and another in long-distance transport. It is also possible that, in this class, the mutants are simply "slow movers" in *N. edwardsonii* and cowpea, and this restricted movement may give the host more time to mount an effective defense. However, as discussed below, this explanation cannot account for all of the phenotypes detected with mutant viruses 204 and 305.

The intermediate phenotypic class, comprising RCNMV MP mutants 204 and 305, does not appear to have a serious defect in cell-to-cell movement and has also retained the capacity to establish wild-type level infections within the CC-SE complex of *N. edwardsonii* lamina on the inoculated leaves. But, interestingly, this capacity did not extend to the phloem (CC-SE complex) of the petiole of the inoculated leaf, as the level of immunogold label in these cells was quite sparse relative to that detected in wild-type RCNMV-infected *N. edwardsonii* plants. In cowpea, these same RCNMV MP mutants were clearly impaired in their capacity to enter into, and/or replicate within, the CC-SE complex of the primary leaf. Presumably as a consequence of the reduced level of virus available for export in the phloem translocation stream, the level of these RCNMV MP mutants detected in the CC-SE in the petiole was extremely low. A similar situation has been reported for plants infected by the mild strain of TMV (Ding *et al.,* 1995b).

All cell types examined in the trifoliolate (uninoculated) leaves of cowpea were free from infection by RCNMV MP mutants 204 and 305, whereas in *N. edwardsonii,* the presence of virus was confined to a limited number of CC-SE in both the petiole and the lamina of the upper leaves (Table 2). Thus, in *N. edwardsonii,* RCNMV MP mutants 204 and 305 are not defective in cell-to-cell movement within the cells of the inoculated leaf, but they are clearly deficient in facilitating (sustaining) entry of infectious material into and/or exit from the phloem translocation stream. This is supported by the fact that mutations 204 and 305 did not delay the appearance of symptoms on the inoculated leaves of infected plants relative to wild type (Table 1). However, these MP mutants react somewhat differently in cowpea, as either mutation in the MP causes a reduction in the ability of the mutant to move into the CC-SE of the lamina in the inoculated leaves. As in the case for RCNMV mutants 27–31/305 and 27–31, it is possible that these mutants are just "slow movers" in cowpea, and the effect on long-distance transport is, at least in part, indirect. An alternate explanation is that these two mutants are impaired in a function required for entry into the CC-SE complex of the inoculated leaves that is distinct from cell-to-cell movement through nonvascular tissues.

TABLE 3

Analysis of the Cell Types in *Nicotiana tabacum* Leaves That Were Infected by Wild-Type RCNMV

Cell type	Level of RCNMV infection[a]
Mesophyll	++++
Bundle sheath	++++
Phloem parenchyma	+++
Companion cell	+(−)
Sieve element	−

[a] Data based on transmission electron microscopic immunogold cytochemical detection of RCNMV CP. Relative level of RCNMV infection determined by immunolocalization of RCNMV CP; symbols as described in Table 2.

The MP mutant phenotypes reveal a role for the RCNMV MP in long-distance transport, specifically in facilitating entry of the virus into the vascular system. This role, at least in the case of MP mutants 204 and 305 in *N. edwardsonii,* is genetically distinct from the MP function in cell-to-cell movement. A similar situation has been reported for TEV (Cronin *et al.,* 1995). However, the phenotype of MP mutants 27–31 and 27–31/305 suggests that the roles of the MP in cell-to-cell movement and long-distance transport may be cumulative or synergistic. Although in a few cases mutant viruses 204 and 305 did achieve a systemic infection in either cowpea or *N. edwardsonii,* respectively (Table 1), they did so at a reduced frequency compared with wild-type RCNMV. The systemic symptoms induced by the mutants in these cases were also milder and appeared on fewer leaves than with the wild-type virus (D. Geisman-Cookmeyer and S. A. Lommel, unpublished results). It is possible that the impaired long-distance transport functions of these MP mutants make it easier for the host to mount a defense response and thus decrease the likelihood of establishing a systemic infection. If this were the case, environmental variables such as temperature and light may well have a significant influence over the outcome of the infection process and could explain variations between individual inoculation experiments.

The RCNMV CP also plays a role in long-distance

FIG. 5. Subcellular localization of RCNMV CP in companion cells and sieve elements of third-order veins located within uninoculated (upper) leaves of *N. edwardsonii* (A–D) and cowpea (E–H) plants infected with RCNMV expressing wild-type and mutant forms of the MP (21 dpi). Immunogold labeling was as in Fig. 3, except that 20-nm gold was employed in G and H. (A and B) Wild-type RCNMV infected CC and SE, respectively. (C and D) RCNMV MP mutant 204 infected CC and SE, respectively. (E and F) Wild-type RCNMV infected CC and SE, respectively. (G and H) RCNMV MP mutant 27–31 infected CC and SE, respectively. Bars, 250 nm, except in A (bar, 300 nm) and F (bar, 400 nm).

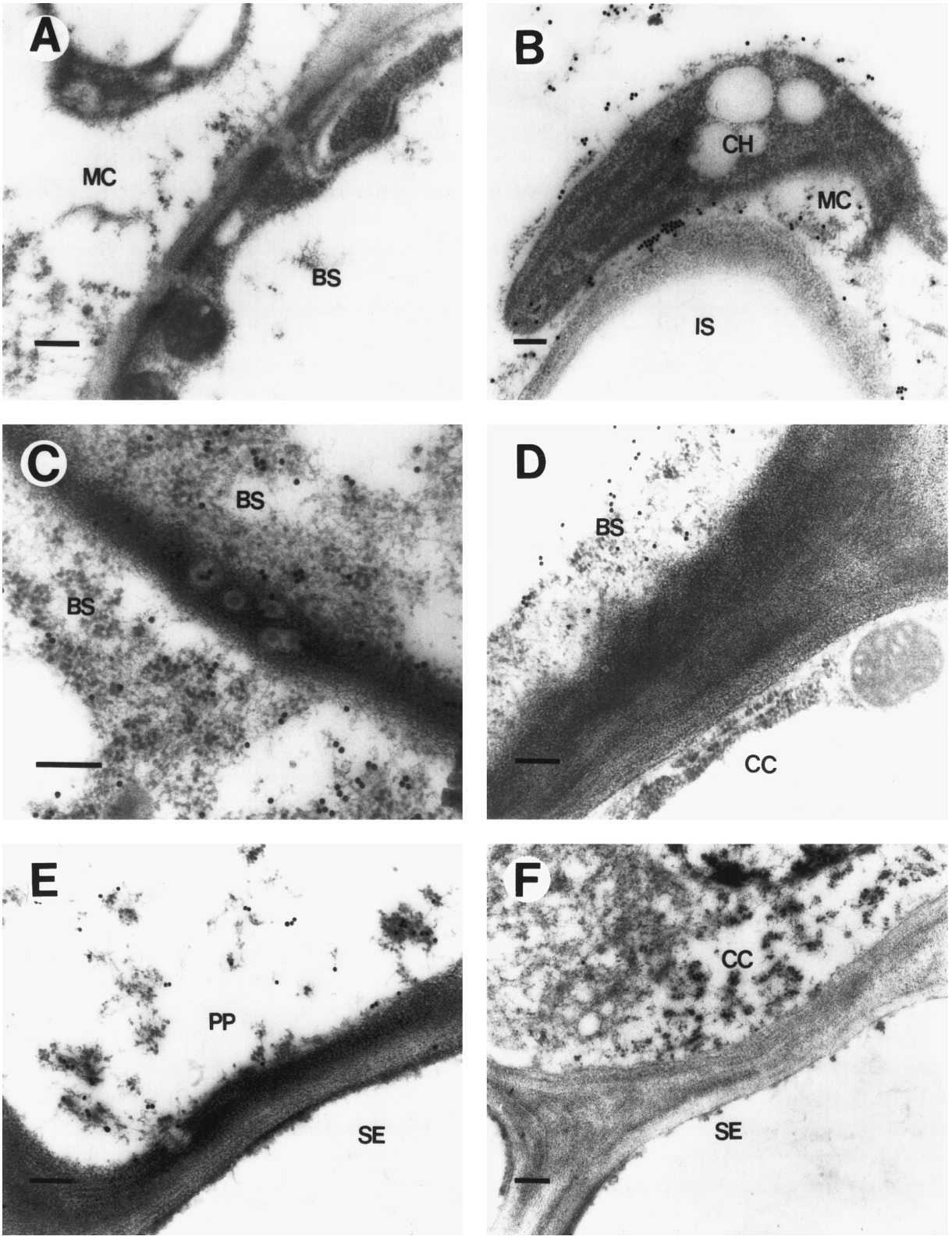

FIG. 6. Subcellular localization of RCNMV CP in different cells within inoculated leaves of *N. tabacum* cv. Xanthi plants infected with wild-type RCNMV (14 dpi). Immunogold labeling was as in Fig. 3, except that 20-nm gold particles were employed throughout. (A) Electron micrograph of mesophyll and bundle sheath cells labeled with preimmune antisera. (B) Electron micrograph of mesophyll cell with RCNMV CP labeled in the cytoplasm. Note the absence of gold label within the chloroplast (CH), the cell wall, and the intercellular space (IS). (C–F). Cellular location of immunogold label within bundle sheath (C and D) and phloem parenchyma (E) cells of a third-order vein. Note the absence of gold label within companion cells (D and F) and sieve elements (E and F). Bars, 200 nm.

transport (Xiong *et al.,* 1993a). Results from the present study suggest that the CP may act at the same cellular location to facilitate systemic infection. In *N. tabacum,* a host where wild-type RCNMV is only able to move from cell to cell and does not cause a systemic infection, we established that the virus does not replicate in the CC of veins located within the inoculated leaves. This raises the possibility that the RCNMV MP and CP act, in a host-specific manner, to potentiate the trafficking of the infectious agent from either the bundle sheath or phloem parenchyma cells into the CC-SE complex. Once in the CC, entry of RCNMV into the phloem translocation stream may require additional host and/or viral factors (Lucas and Gilbertson, 1994; Ding *et al.,* 1995a; Gilbertson and Lucas, 1996). Thus, an incompatibility between either the RCNMV MP and/or CP and the host would prevent successful viral entry into the long-distance transport pathway. Future experiments will address the roles played by both the RCNMV MP and CP in potentiating systemic infection.

MATERIALS AND METHODS

Plant inoculations

Wild-type and mutant RCNMV RNAs were transcribed from *Sma*I linearized templates as previously described (Xiong and Lommel, 1991; Giesman-Cookmeyer and Lommel, 1993). RNA (produced from a 300-ml reaction mixture) in GKP buffer (50 mM glycine, 30 mM K_2HPO_4, pH 9.2, 1% bentonite, 1% celite) was used to inoculate a total of four leaves on two *N. edwardsonii, V. unguiculata* cv. California Blackeye (cowpea), or *N. benthamiana* plants. For *Nicotiana* species, a pair of the next to oldest set of leaves was inoculated when plants were at the six- to eight-leaf stage. For cowpea, the primary leaves were inoculated before the appearance of the first trifoliolate leaves. Mutant RNA-2 transcripts were co-inoculated with wild-type RNA-1 transcript. Each set of mutants was inoculated onto two plants and assayed in three separate experiments. Plants were maintained under normal greenhouse conditions.

For immunolocalization (fluorescence and gold labeling) studies, desiccator-dried tissue from *N. benthamiana* plants infected with the wild-type and MP mutants were used to infect *N. edwardsonii,* cowpea, and *N. benthamiana* plants. For these inoculations, tissue was ground with a mortar and pestle in 3 ml of 10 mM phosphate-buffered saline, pH 7.0. A cotton-tipped applicator was used to apply sap to equivalent leaves on plants at the same developmental status as described above for infection assays. At least 10 plants of each species were used per viral infection treatment and all were maintained in a greenhouse under a day/night temperature regime of 25 and 18°C, respectively.

Tissue fixation and immunolocalization protocols

Plant tissues from the inoculated leaves were collected at 14 days postinoculation (dpi) and from uninoculated (upper) leaves at 21 dpi. Wild-type RCNMV normally develops systemic symptoms 4–7 dpi, but, to allow for the possibility that the mutants under study may move more slowly, plants were analyzed at the later time points. Samples included the petiole as well as the main to the fourth-order veins. Tissues were fixed in 1.25% (w/v) glutaraldehyde and 3% (w/v) paraformaldehyde in 100 mM phosphate buffer (pH 7.2) for 3–4 h at room temperature. After four 15-min washes in 100 mM phosphate buffer (pH 7.0) at 4°C, the tissue samples were dehydrated through a 10% step-graded ethanol series at 4°C; each step was for 15 min, and the final 100% ethanol step incorporated three 15-min changes. Tissue infiltration was carried out over 2 days through a five-step graded series from 100% ethanol to 100% London resin (LR) White (medium grade; Electron Microscopy Sciences), and then embedded in LR White resin. Blocks were polymerized by exposure to a temperature sequence of 40°C for 12 h, 50°C for 12 h, and 60°C for 35 h.

For immunolocalization studies performed at the light microscope level, semi-thin sections (500–750 nm) were cut on a glass knife and then transferred to and dried onto 1.5-cm-diameter wells fabricated using Slipknot Vinyl Tape (No. 44; Plymouth Rubber Co., Inc., Canton, MA) that was attached to superfrost/plus microscope slides (Fisher Scientific Co., Pittsburgh). Sections were preincubated in 100 μl blocking solution [50 mM Tris–HCl, 150 mM NaCl, pH 7.4, 2% (w/v) bovine serum albumin (BSA; Fisher Scientific Co.) and 0.1% (v/v) Tween 20] for 1 h. Sections were then incubated for 3 h in appropriate antisera (preimmune or RCNMV CP) diluted 1:200 in antibody diluent [50 mM Tris–HCl, 150 mM NaCl, pH 7.4, 0.1% (w/v) BSA, 0.1% (v/v) Tween 20, and 0.02 % (w/v) sodium azide]. The polyclonal antibody raised against the RCNMV CP was developed in rabbit by intramuscular injection of SDS–PAGE-purified RCNMV CP (Xiong *et al.,* 1993b). After four 15-min washes with blocking solution, sections were incubated for 1 h in biotin-XX goat anti-rabbit IgG [H + L] (Molecular Probes) diluted 1:50 with antibody diluent, followed by three washes for 15 min each with blocking solution. Sections were then labeled using ELF (Enzyme-Labeled-Fluorescence)-97 Cytological Labeling kit 2 according to the instructions provided by the manufacturer (Molecular Probes). Sections were then stained with 0.05% (w/v) Safranin O for 2 min to enable the identification of cell types.

After a washing in glass-distilled water, ELF sections were immersed in Mounting medium (provided by the Kit) and Safranin O fluorescence was visualized on a Leica confocal laser-scanning microscope (Model TCS-4D CLSM, Leica Lasertechnik GmbH, Heidlberg, Germany) using a krypton/argon laser and the two-channel scanning

mode. The first channel was used to detect green fluorescence (488-nm excitation and 507-nm emission filters), while the second channel detected red fluorescence (568-nm excitation and 590-nm emission filters). The green fluorescent signal associated with the ELF reporter used to identify the cellular location of the RCNMV CP was detected using a UV laser (363-nm excitation and 515-nm emission filters). More than 50 sections were examined for each viral infection treatment and the distribution of ELF was recorded. Images were directly recorded in TIFF format at a PC workstation and processed with Adobe Photoshop (Version 3.0.4). After generation of pseudocolors, photographic images were printed via a Tektronix phase 440 laser printer. Note that in addition to autofluorescence associated with the xylem conducting tissue, ELF signal, due to nonspecific binding of the RCNMV CP, was detected in these same cell types.

For subcellular immunogold localization of RCNMV CP, ultrathin sections (70–80 nm) were cut with a diamond knife and collected on uncoated mesh grids or Formvar film-coated slot grids. The procedures employed for immunolabeling were similar to those described for fluorescence-based detection, but with the following modifications. Sections were treated in appropriate antisera, at dilutions of 1:1000, followed by three 15-min washes with blocking solution before being incubated for 1 h in secondary antibody (15- or 20-nm-diameter gold-conjugated goat anti-rabbit IgG) diluted 1:50 in antibody diluent. Sections were then given three 10-min washes in antibody diluent, blocking solution, and double-distilled water to remove unbound secondary antibody. Sections were then stained with uranyl acetate (2% w/v in distilled water) followed by lead citrate, each for 10 min, and then observed using a JEOL 100S-A electron microscope operated at 80 kV. For these studies, six blocks were prepared per infected plant and between 50 and 100 grids were prepared and examined, per block, to evaluate the cellular distribution of the RCNMV CP.

ACKNOWLEDGMENTS

This research was supported by NSF Grant IBN-94-06974 (to W.J.L.), USDA NRICGP Grant 93-37303-8929 (to S.A.L.), and NSF Grant MCB-94-19700 (to S.A.L.).

REFERENCES

Atabekov, J. G., and Taliansky, M. E. (1990). Expression of a plant virus-coded transport function by different viral genomes. *Adv. Virus Res.* 38, 201–248.

Carrington, J. C., and Morris, T. J. (1984). Complementary DNA cloning and analysis of carnation mottle virus RNA. *Virology* 139, 22–31.

Carrington, J. C., Kasschau, K. D., Mahajan, S., and Schaad, M. C. (1996). Cell-to-cell and long-distance transport of viruses in plants. *Plant Cell* 8, 1669–1681.

Citovsky, V., Knorr, D., Schuster, G., and Zambryski, P. (1990). The P30 movement protein of tobacco mosaic virus is a single-strand nucleic acid binding protein. *Cell* 60, 637–647.

Citovsky, V., Knorr, D., and Zambryski, P. (1991). Gene1, a potential cell-to-cell movement locus of cauliflower mosaic virus, encodes an RNA binding protein. *Proc. Natl. Acad. Sci. USA* 88, 2476–2480.

Cronin, S., Verchot, J., Haldeman-Cahill, R., Schaad, M. C., and Carrington, J. C. (1995). Long-distance movement factor: A transport function of the potyvirus helper component proteinase. *Plant Cell* 7, 549–559.

Dawson, W. O., and Hilf, M. E. (1992). Host-range determinants of plant viruses. *Annu. Rev. Plant Physiol. Plant Mol. Biol.* 43, 527–555.

Deom, C. M., Lapidot, M., and Beachy, R. N. (1992). Plant virus movement proteins. *Cell* 69, 221–224.

Ding, B., Haudenshield, J. S., Hull, R. J., Wolf, S., Beachy, R. N., and Lucas, W. J. (1992). Secondary plasmodesmata are specific sites of localization of the tobacco mosaic virus movement protein in transgenic tobacco plants. *Plant Cell* 4, 915–928.

Ding, S.-W., Li, W.-X., and Symons, R. H. (1995a). A novel naturally occurring hybrid gene encoded by a plant RNA virus facilitates long distance virus movement. *EMBO J.* 14, 5762–5772.

Ding, X. S., Shintaku, M. H., Arnold, S. A., and Nelson, R. S. (1995b). Accumulation of mild and severe strains of tobacco mosaic virus in minor veins of tobacco. *Mol. Plant–Microbe Interact.* 8, 32–40.

Ding, B., Li, Q., Nguyen, L., Palukaitis, P., and Lucas, W. J. (1995c). Cucumber mosaic virus 3a protein potentiates cell-to-cell trafficking of CMV RNA in tobacco plants. *Virology* 207, 345–353.

Fujiwara, T., Giesman-Cookmeyer, D., Ding, B., Lommel, S. A., and Lucas, W. J. (1993). Cell-to-cell trafficking of macromolecules through plasmodesmata potentiated by the red clover necrotic mosaic virus movement protein. *Plant Cell* 5, 1783–1794.

Giesman-Cookmeyer, D., and Lommel, S. A. (1993). Alanine scanning mutagenesis of a plant virus movement protein identifies three functional domains. *Plant Cell* 5, 973–982.

Gilbertson, R. L., and Lucas, W. J. (1996). How do viruses traffic on the 'vascular highway'? *Trends Plant Sci.* 1, 260–267.

Ghoshroy, S., Lartey, E., Sheng, J., and Citovsky, V. (1997). Transport of proteins and nucleic acids through plasmodesmata. *Annu. Rev. Plant Physiol. Plant Mol. Biol.* 48, 27–50.

Goodrick, B. J., Kuhn, C. W., and Hussey, R. S. (1991). Restricted systemic movement of cowpea chlorotic mottle virus in soybean with nonnecrotic resistance. *Phytopathology* 81, 1426–1431.

Hilf, M. E., and Dawson, W. O. (1993). The tobamovirus capsid protein functions as a host-specific determinant of long-distance movement. *Virology* 193, 106–114.

Hull, R. (1991). The movement of viruses within plants. *Semin. Virol.* 2, 89–95.

Lucas, W. J. (1995). Plasmodesmata: Intercellular channels for macromolecular transport in plants. *Curr. Opin. Cell. Biol.* 7, 673–680.

Lucas, W. J., and Wolf, S. (1993). Plasmodesmata: The intercellular organelle of green plants. *Trends Cell Biol.* 3, 308–315.

Lucas, W. J., and Gilbertson, R. L. (1994). Plasmodesmata in relation to viral movement within leaf tissues. *Annu. Rev. Phytopathol.* 32, 387–422.

Maniatis, T., Fritsch, E. F., and Sambrook, J. (1982). "Molecular Cloning: A Laboratory Manual" Cold Spring Harbor Laboratory, Cold Spring Harbor, NY.

Maule, A. J. (1991). Virus movement in infected plants. *Crit. Rev. Plant Sci.* 9, 457–473.

Noueiry, A. O., Lucas, W. J., and Gilbertson, R. L. (1994). Two proteins of a plant DNA virus coordinate nuclear and plasmodesmal transport. *Cell* 76, 925–932.

Nguyen, L., Lucas, W. J., Ding, B., and Zaitlin, M. (1996). Viral RNA trafficking is inhibited in replicase-mediated resistant transgenic tobacco plants. *Proc. Natl. Acad. Sci. USA* 93, 12643–12647.

Osman, T. A. M., Hayes, R. J., and Buck, K. W. (1992). Cooperative binding of the red clover necrotic mosaic virus movement protein to single-stranded nucleic acids. *J. Gen. Virol.* 73, 223–227.

Ragetli, H. W. J., and Elder, M. (1977). Characteristics of clover primary leaf necrosis virus, a new spherical isolated from *Trifolium pratense*. *Can. J. Bot.* 55, 2122–2136.

Rojas, M. R., Zerbini, F. M., Allison, R. F., Gilbertson, R. L., and Lucas, W. J. (1997). Capsid protein and helper component-proteinase function as potyvirus cell-to-cell movement proteins. *Virology* 237, 283–295.

Schaad, M. C., and Carrington, J. C. (1996). Suppression of long distance movement of tobacco etch virus in a nonsusceptible host. *J. Virol.* 70, 2556–2561.

Schoumacher, F., Erny, C., Berna, A., Godefroy-Colburn, T., and Stussi-Garaud, C. (1992). Nucleic acid-binding properties of the alfalfa mosaic virus movement protein produced in yeast. *Virology* 188, 896–899.

Sudarshana, M. R., Wang, H. L., Lucas, W. J., and Gilbertson, R. L. (1998). Dynamics of bean dwarf mosaic geminivirus cell-to-cell and long-distance movement in *Phaseolus vulgaris* revealed using the green fluorescent protein. *Mol. Plant-Microbe Interact.,* 11, 277–291.

Waigmann, E., Lucas, W. J., Citovsky, V., and Zambryski, P. (1994). Direct functional assay for tobacco mosaic virus cell-to-cell movement protein and identification of a domain involved in increasing plasmodesmal permeability. *Proc. Natl. Acad. Sci. USA* 91, 1433–1437.

Waigmann, E., and Zambryski, P. (1995). Tobacco mosaic virus movement protein-mediated transport between trichome cells. *Plant Cell* 7, 2069–2079.

Wang, H. L., Gilbertson, R. L., and Lucas, W. J. (1996). Spatial and temporal distribution of bean dwarf mosaic geminivirus in *Phaseolus vulgaris* and *Nicotiana benthamiana. Phytopathology* 86, 1204–1214.

Wolf, S., Deom, C. M., Beachy, R. N., and Lucas, W. J. (1989). Movement protein of tobacco mosaic virus modifies plasmodesmatal size exclusion limit. *Science* 246, 377–379.

Xiong, Z., Kim, K. H., Giesman-Cookmeyer, D., and Lommel, S. A. (1993a). The roles of the red clover necrotic mosaic virus capsid and cell-to-cell movement proteins in systemic infection. *Virology* 192, 27–32.

Xiong, Z., Kim, K. H., Kendall, T. L., and Lommel, S. A. (1993b). Synthesis of the putative red clover necrotic mosaic virus RNA polymerase by ribosomal frameshifting *in vitro. Virology* 193, 213–221.

Xiong, Z., and Lommel, S. A. (1991). Red clover necrotic mosaic virus infectious transcripts synthesized *in vitro. Virology* 182, 388–392.